Journal of Integrative Neuroscience

J. Integr. Neurosci. **2026**; 25(10): 52364
https://doi.org/10.31083/JIN52364

Short Communication

Smad4 Regulates the Developmental Coordination of Cortical Neurons via the CXCL12-CXCR4 Axis

Yuan Wang[1], Yao Zhang[1], Yuanyuan Li[1], Wenzhuo Han[1], Baoqian Shan[1], Youming Wang[1], Bin Chen[2,*], Rongliang Guo[1,3,*]

[1]School of Clinical Medicine, Hebei University of Engineering, 056038 Handan, Hebei, China
[2]Department of Rehabilitation Medicine, The Affiliated People's Hospital of Fujian University of Traditional Chinese Medicine, 350004 Fuzhou, Fujian, China
[3]Department of Central Laboratory, Affiliated Hospital of Hebei University of Engineering, 056038 Handan, Hebei, China
*Correspondence: chenbin327425224@163.com (Bin Chen); rlguo20@fudan.edu.cn (Rongliang Guo)
Academic Editor: Hajime Hirase
Submitted: 28 March 2026 Revised: 14 May 2026 Accepted: 26 May 2026 Published: 13 October 2026

Abstract

Background: The functional assembly of neural circuits during cortical development relies on the precise spatiotemporal coordination of excitatory projection neurons and inhibitory interneurons. Here, we show that SMAD family member 4 (SMAD4) is required for this developmental coordination. **Methods:** We performed conditional deletion of *Smad4* in pallial progenitors and evaluated the spatial distribution and number of Glutamic acid decarboxylase 67-green fluorescent protein positive (*Gad67*-GFP^{+}) interneurons in the embryonic and adult cortex. Single-cell RNA sequencing (scRNA-seq) was utilized to assess transcriptomic changes in the *Smad4*-deficient cortex. Further *in vivo* expression validation and functional assessments were conducted using a C-X-C motif chemokine ligand 12 (*Cxcl12*)-Discosoma red fluorescent protein (DsRed) reporter line and *Cxcl12* loss-of-function mutants, respectively. **Results:** Conditional deletion of *Smad4* in pallial progenitors disrupts the spatial distribution and overall number of *Gad67*-GFP+ interneurons in both the embryonic and adult cortex. scRNA-seq revealed a marked reduction in *Cxcl12* expression within the mutant cortex, while its receptor, C-X-C chemokine receptor type 4 (*Cxcr4*), remained normally expressed in interneurons. We confirmed this downregulation *in vivo* using the *Cxcl12*-DsRed reporter line. Functionally, *Cxcl12* loss-of-function mutants phenocopy the interneuron migration deficits seen in *Smad4* mutants. **Conclusions:** Our results uncover a projection neuron-derived SMAD4-CXCL12 signaling cascade that regulates CXCR4-dependent interneuron migration, providing a molecular basis for the cross-talk between these two distinct neuronal lineages.

Keywords: Smad4; cortical development; interneuron migration; CXCL12; CXCR4

1. Introduction

Mammalian cerebral cortex development involves the orchestrated integration of locally generated excitatory projection neurons (PNs) and inhibitory interneurons (INs), which migrate long distances from the ganglionic eminences [1,2,3]. The proper assembly of cortical circuits depends heavily on the coordinated development of these two distinct lineages [4,5]. While several extrinsic guidance cues are known, the intrinsic mechanisms by which PNs influence and coordinate IN migration are still not fully understood. SMAD family member 4 (*Smad4*) serves as a central intracellular mediator with critical roles in early neurodevelopment [6,7,8]. Despite its broad developmental functions, the specific cell-autonomous and non-cell-autonomous roles of *Smad4* in organizing the interplay between PNs and INs remain largely unexplored [8,9]. In this study, we report that deleting *Smad4* specifically in PNs severely impairs IN distribution. We further show that this defect is driven by the targeted downregulation of the chemokine C-X-C motif chemokine ligand 12 (CXCL12), which disrupts the CXCL12-C-X-C chemokine receptor type 4 (CXCR4) guidance axis.

2. Materials and Methods

2.1 Mice

The mouse lines (The Jackson Laboratory, Bar Harbor, ME, USA) used in this study, including *Smad4* (JAX no. 017462) [10], Emx1-Cre (JAX no. 005628) [11,12], Gad67-GFP (JAX no. 003718) [13], and Cxcl12-DsRed (JAX no. 022458) [14], have been described previously. Control mice consisted of both wild-type (WT) and Cre-negative littermates from the same crosses, ensuring an equivalent genetic background across all experimental groups. The day a vaginal plug was detected was designated as embryonic day 0.5 (E0.5), and the day of birth was designated as postnatal day 0 (P0). The sexes of the embryonic and early postnatal mice were not distinguished for these experiments.

2.2 Tissue Preparation

Embryos were isolated from pregnant mice deeply anesthetized via intraperitoneal injection of pentobarbital sodium (100 mg/kg, P3761, Sigma-Aldrich, Darmstadt, Germany). Embryonic brains were dissected and fixed overnight in 4% paraformaldehyde (PFA, A500684, San-

Copyright: © 2026 The Author(s). Published by IMR Press.
This is an open access article under the CC BY 4.0 license.

Publisher's Note: IMR Press stays neutral with regard to jurisdictional claims in published maps and institutional affiliations.

gon Biotech, Shanghai, China) prepared in diethylpyrocarbonate (DEPC)-treated water (B600154, Sangon Biotech). Postnatal mice were deeply anesthetized via intraperitoneal injection of pentobarbital sodium and transcardially perfused with phosphate-buffered saline (PBS), followed by 4% PFA. All dissected brains were post-fixed overnight in 4% PFA at 4 °C, then cryoprotected by dehydration in 30% sucrose for at least 24 hours. The tissues were embedded in optimal cutting temperature (OCT) compound (4583, Sakura Finetek, Tokyo, Japan), stored at –80 °C, and subsequently sectioned into 20-µm-thick coronal slices for analysis.

2.3 Euthanasia

Animals were deeply anesthetized by intraperitoneal injection of pentobarbital sodium (100 mg/kg). After the loss of consciousness and absence of pedal withdrawal reflex, euthanasia was confirmed by cervical dislocation. All animal procedures were performed in accordance with the institutional animal care and use committee guidelines.

2.4 Immunofluorescence

Immunofluorescence staining was conducted on 10-µm or 20-µm cryosections following standard laboratory protocols [15]. Briefly, sections were rinsed in Tris-buffered saline (TBS; 0.01 M Tris–HCl, 0.9% NaCl, pH 7.4) for 10 min and permeabilized with 0.5% Triton X-100 in TBS for 30 min at room temperature (RT). The sections were then blocked in 5% donkey serum combined with 0.5% Triton X-100 in TBS (pH 7.2) for 2 hours at RT. Guinea pig anti-EOMES (TBR2, 1:500, Oasis Biofarm, OBPGP022, Hangzhou, Zhejiang, China), diluted in the blocking buffer, were applied overnight at 4 °C. The following day, sections were washed three times in TBS (10 min each) and incubated with species-matched fluorescent secondary antibodies (Jackson ImmunoResearch; 1:500 dilution) for 2 hours at RT in the dark. After three final TBS washes, nuclei were counterstained with 4′,6-diamidino-2-phenylindole (DAPI; Sigma, 200 ng/mL in TBS) for 2 min, and the sections were then cover-slipped with Gel/Mount (Biomeda).

2.5 scRNA-seq Data Analysis

Raw sequencing reads were aligned to the mm10 mouse reference genome and quantified using the Cell Ranger pipeline (v.7.1.0; 10x Genomics, Pleasanton, CA, USA). The resulting count matrices were processed using the 'Seurat' R package (v.5.1.0, Satija Lab, New York, NY, USA; https://satijalab.org/seurat/). For each experimental group (Control and *Smad4*-ECKO), cortical tissues from two independent E14.5 embryos were pooled to generate a single-cell library. This pooling strategy was utilized to minimize inter-individual biological variation and ensure a robust, representative transcriptional profile for each condition. Batch-specific quality control (QC) thresholds were applied to account for variations in sequencing depth. Low-quality cells—defined as having an abnormally low number of unique molecular identifiers (UMIs) or a high percentage of mitochondrial gene-derived UMIs—were filtered out. Doublets were predicted and removed using the DoubletFinder package (v2.0; https://github.com/chris-mcginnis-ucsf/DoubletFinder).

Following QC, gene expression data were log-normalized, and the top 3000 highly variable genes were identified using the "vst" method. To mitigate technical variations and effectively harmonize the datasets across different conditions, we implemented the IntegrateLayers function within the Seurat v5 framework. Principal component analysis (PCA) was performed **on the integrated data**, and the top 50 principal components were used for neighborhood graph construction and unsupervised clustering. UMAP was utilized for low-dimensional visualization. Differentially expressed genes (DEGs) across clusters were identified via the Wilcoxon rank-sum test, with *p* values adjusted using the Benjamini–Hochberg false discovery rate (FDR) correction.

The scRNA-seq libraries were sequenced on an Illumina NovaSeq 6000 platform. For the Control group, sequencing yielded 344.5 million total reads, with a mean of 25,586 reads per cell. After quality control filtering, 13,311 cells were retained, featuring a median of 1990 genes detected per cell. For the *Smad4*-ECKO group, sequencing yielded 411.6 million total reads, with a mean of 29,808 reads per cell. After filtering, 13,647 cells were retained, featuring a median of 2067 genes detected per cell.

It should be noted that cortical tissues from two embryos were pooled to generate a single scRNA-seq library per condition; thus, the statistical significance derived from cell-level transcriptomic comparisons primarily reflects cellular-level variances and should be interpreted with caution regarding biological replication.

2.6 Image Acquisition and Analysis

Fluorescence images were acquired using an ImageXpress Micro 4 Automated Slide Scanner (at 10× or 20× magnification). Images were processed using Adobe Photoshop and Illustrator (Adobe Systems, San Jose, CA, USA) for clarity, optimal contrast, and panel assembly, without altering the integrity of the original raw data.

2.7 Quantification and Statistical Analysis

Quantitative analyses of fluorescence images were performed using ImageJ software (National Institutes of Health, Bethesda, MD, USA). Statistical analyses were executed utilizing GraphPad Prism 10 (Dotmatics, Boston, MA, USA). For *in vivo* histological quantifications, the biological replicate was strictly defined as an individual animal (n = 4 independent mice per genotype, unless otherwise specified). To ensure representative sampling and account for intra-individual anatomical variance, four

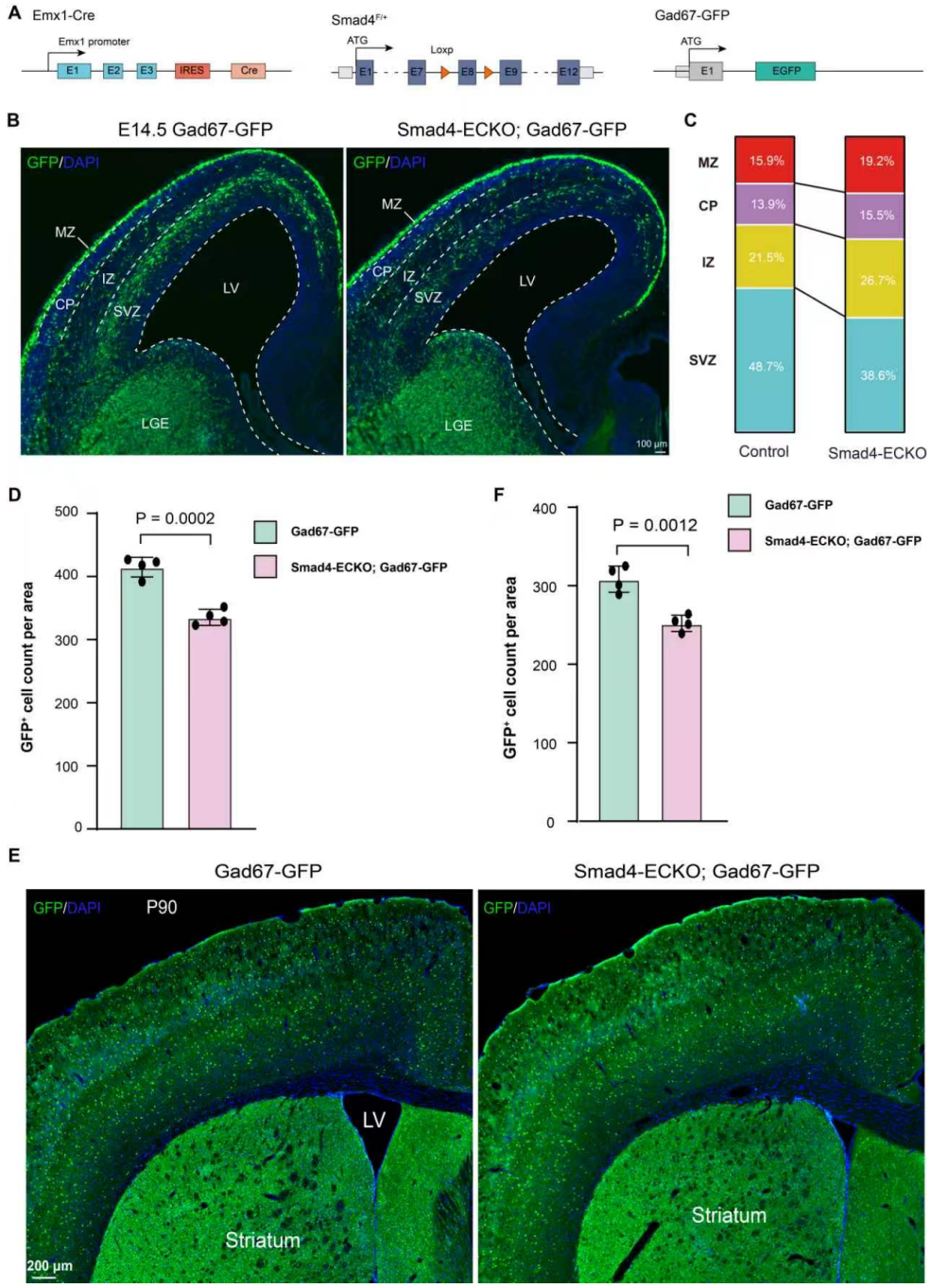


Fig. 1. Deletion of *Smad4* disrupts the distribution and number of cortical interneurons. (A) Schematic illustration of the genetic strategy used to generate the Emx1-Cre, *Smad4*$^{F/+}$, and Gad67-GFP mouse lines. (B) Representative immunofluorescence images showing the distribution of Gad67-GFP^{+} interneurons in the embryonic day 14.5 (E14.5) cortices of control (Gad67-GFP) and *Smad4*-ECKO (Emx1-Cre; *Smad4*$^{F/F}$; Gad67-GFP) mice. The dashed lines indicate the boundary between the LV and the cortex. Scale bar = 100 μm. (C) Quantification of the proportional distribution of Gad67-GFP^{+} cells across different cortical zones in control and *Smad4*-ECKO mice. (D) Bar graph showing the total number of GFP^{+} cells per defined area in the E14.5 cortices of control and *Smad4*-ECKO mice. (E) Representative immunofluorescence images showing the distribution of Gad67-GFP^{+} cells in the adult (postnatal day 90, P90) cortices of control and *Smad4*-ECKO mice. Scale bar = 200 μm. (F) Quantification of the total number of GFP^{+} cells per defined area in the P90 cortices. Data are presented as mean ± SEM (n = 4 mice per group); unpaired Student's *t*-test. Abbreviations: IRES, internal ribosome entry site; EGFP, enhanced green fluorescent protein; Smad4, SMAD family member 4; Emx1-Cre, Empty spiracles homeobox 1-Cre recombinase; Gad67-GFP, Glutamic acid decarboxylase 67-green fluorescent protein; ECKO, Emx1-Cre conditional knockout; P90, Postnatal day 90; DAPI, 4′,6-diamidino-2-phenylindole; MZ, marginal zone; CP, cortical plate; IZ, intermediate zone; SVZ, subventricular zone; LGE, lateral ganglionic eminence; LV, Lateral ventricle.

matched coronal sections at identical rostro-caudal levels were selected and analyzed per mouse. The cell counts or fluorescence intensities from these four sections were averaged to generate a single data point per biological replicate.

Consistent with our established laboratory protocols for developmental studies, statistical significance between the Control and mutant groups was determined using an unpaired Student's *t*-test. All quantitative data are presented as mean ± SEM (standard error of the mean). Exact *p*-values are explicitly reported in the corresponding results text and figure legends. A $p < 0.05$ was considered statistically significant. The specific quantification criteria were as follows:

2.7.1 Cell Counting

Quantification of GFP^+ interneurons was performed in the putative somatosensory and motor cortices of E14.5 and P90 mice across Control and *Smad4*-ECKO groups. High-resolution images of coronal sections were acquired using an Olympus VS120 Automated Slide Scanner (10× objective, Olympus, Tokyo, Japan). For each biological replicate (n = 4 mice per genotype), four anatomically matched sections at identical rostro-caudal levels were analyzed. Within each section, GFP^+ cells were quantified using a standardized radial column (1000-pixel bin width) spanning the entire neuroepithelial thickness from the ventricular zone (VZ) to the marginal zone (MZ) or pial surface (Fig. 1C,D,F). Identical standardized counting procedures were applied to the Cxcl12 loss-of-function model (Cxcl12-DsRed/DsRed; Gad67-GFP) at E15.5 (Fig. 3E).

2.7.2 Fluorescence Intensity and Normalization

To assess CXCL12 protein levels, DsRed immunofluorescence intensity was measured in the E14.5 cortices of Control and *Smad4*-ECKO; Cxcl12-DsRed mice. For each animal, 4 matched coronal sections were processed, and the raw signal intensities were normalized to the mean of the Control group to account for inter-individual variation (Fig. 3C). Statistical significance was determined using the unpaired Student's *t*-test. All quantitative data are presented as mean ± SEM, with a $p < 0.05$ considered statistically significant. Due to the variability in fluorescence intensity, 6 mice were analyzed for the control group and 8 mice for the experimental group.

3. Results

3.1 Smad4 Deficiency in Projection Neurons Disrupts Interneuron Coordination

To investigate the role of *Smad4* in cortical development, we generated conditional knockout mice (*Smad4*-Emx1-Cre recombinase [Emx1-Cre] conditional knockout [ECKO]) by crossing $Smad4^{F/F}$ with Emx1-Cre, which specifically targets dorsal telencephalic progenitors (Fig. 1A). We introduced the Glutamic acid decarboxylase 67-green fluorescent protein positive (Gad67-GFP) allele to trace interneurons. At embryonic day 14.5 (E14.5), *Smad4*-ECKO mice exhibited a profoundly altered spatial distribution of Gad67-GFP^+ interneurons across the cortical zones compared to control littermates (Fig. 1B). The proportional distribution of interneurons across the marginal zone (MZ), cortical plate (CP), intermediate zone (IZ), and subventricular zone (SVZ) was significantly skewed, accompanied by a marked reduction in the total number of GFP^+ cells per defined area (Fig. 1C,D). Importantly, this cortical reduction was accompanied by a striking ectopic accumulation of interneurons at the pallial-subpallial boundary within the lateral ganglionic eminence (LGE), indicating a primary defect in directed migration. This numerical and spatial deficit persisted into adulthood (postnatal day 90, P90), indicating a permanent disruption of cortical circuit assembly (Fig. 1E,F). Because Emx1-Cre does not directly target interneurons, this non-cell-autonomous defect strongly suggests that *Smad4* expression in PNs is fundamentally required to coordinate IN migration.

3.2 Single-cell RNA Sequencing (scRNA-seq) Reveals CXCL12 as a Primary Downstream Target of Smad4

To elucidate the molecular basis of this coordination failure, we performed scRNA-seq on E14.5 cortices from control and *Smad4*-ECKO mice (Fig. 2A). Unsupervised Uniform Manifold Approximation and Projection (UMAP) clustering resolved 12 distinct transcriptomic populations, each defined by established marker gene signatures (Fig. 2B,C and **Supplementary Table 1**). Specifically, Cluster 4 was annotated as the migrating interneuron population, a classification strictly validated by the robust enrichment of pan-gamma-aminobutyric acid-ergic (GABAergic) markers (*Gad1*, *Gad2*) and lineage-determining genes (Specificity protein 9 [*Sp9*], LIM homeobox 6 [*Lhx6*]) [16,17,18,19] (**Supplementary Fig. 1**). Within the pallial germinal zones, the overall transcriptomic distribution and population sizes of Paired box 6 $(Pax6)^+$ radial glia and Eomesodermin $(Eomes)^+$ intermediate progenitor cells (IPCs) remained unperturbed between the two genotypes (Fig. 2D). To further validate these transcriptomic findings *in vivo*, we performed immunofluorescence staining for EOMES/T-box brain protein 2 (TBR2). Consistent with our scRNA-seq data, the spatial distribution and laminar arrangement of these progenitor populations showed no apparent differences between Control and *Smad4*-ECKO cortices (**Supplementary Fig. 2**), confirming that the glutamatergic progenitor scaffold remains architecturally intact.

It is well established that cortical interneurons, which primarily originate from the medial ganglionic eminence (MGE), express the CXCR4 [20,21] and rely on the IPC-secreted chemokine CXCL12 for directed migration into the pallium [4,22,23]. Strikingly, our data revealed a profound uncoupling of this guidance axis in the mutant cortex: while the $Eomes^+$ IPC pool itself remained quantitatively and structurally intact, its expression of Cxcl12 was drastically and specifically downregulated (Fig. 2E,F).

IMR Press

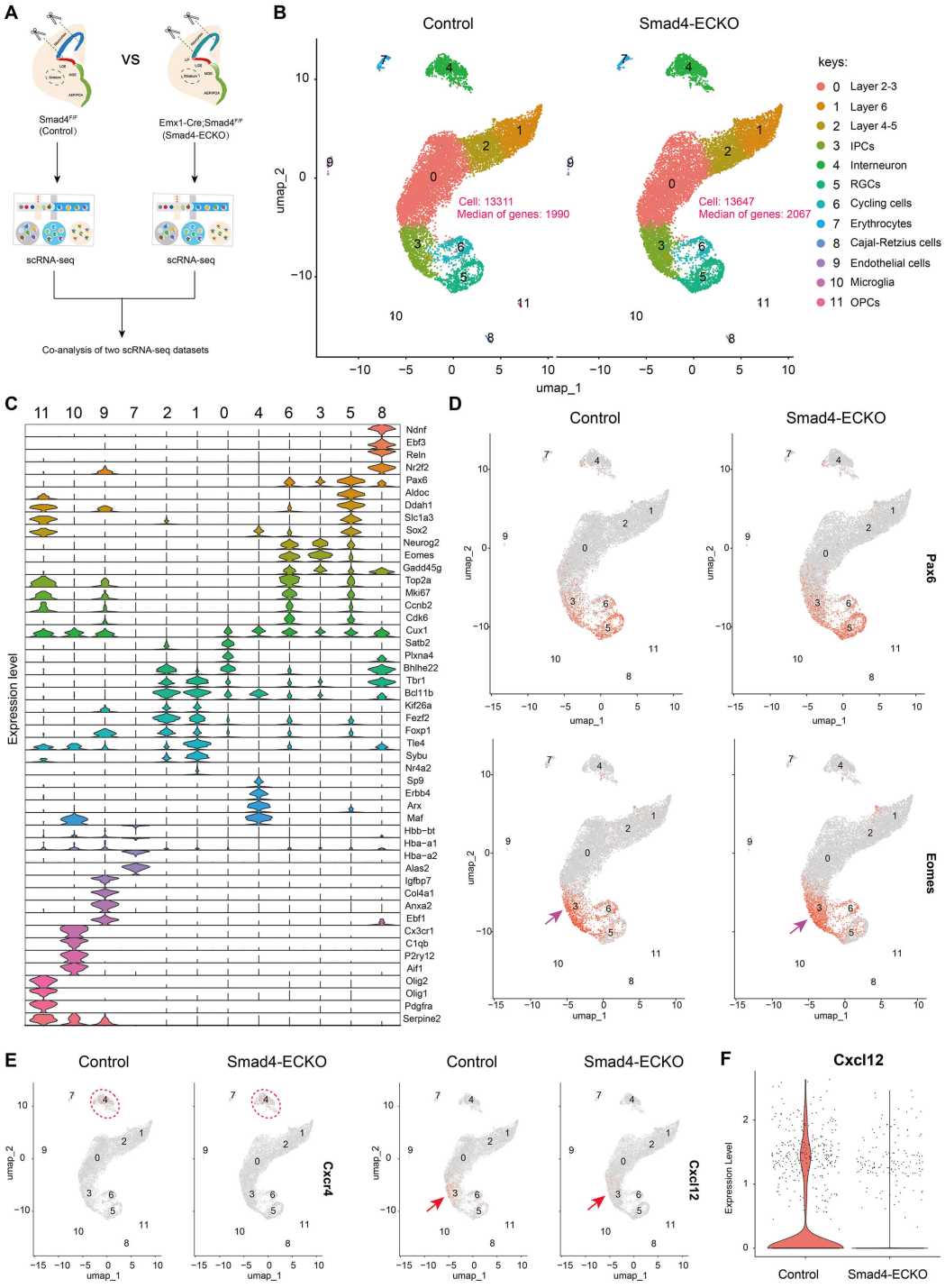


Fig. 2. scRNA-seq reveals downregulation of Cxcl12 in the *Smad4*-deficient cortex. (A) Schematic representation of the scRNA-seq experimental design for control (*Smad4*$^{F/F}$) and *Smad4*-ECKO (Emx1-Cre; *Smad4*$^{F/F}$) cortices. (B) Uniform Manifold Approximation and Projection (UMAP) plots showing the clustering of distinct cell populations (clusters 0–11) from both groups. (C) Violin plots displaying the expression levels of highly differentially expressed marker genes across the identified cell clusters (0–11). (D) UMAP plots showing the distribution and expression of the radial glial cell (RGC) marker Pax6 and the intermediate progenitor cell (IPC) marker Eomes in control and *Smad4*-ECKO groups. (E) UMAP plots reveal that Cxcr4 is predominantly expressed in cortical interneurons, with no significant change in expression between the control and *Smad4*-ECKO groups. In contrast, the expression of Cxcl12 is markedly downregulated in the *Smad4*-ECKO group (indicated by arrows). (F) Violin plot quantifying the significant reduction of Cxcl12 expression in the *Smad4*-ECKO cortex compared to the control. For each group, cortical tissues from 2 independent embryos (n = 2 animals per group) were pooled to generate the single-cell suspension.

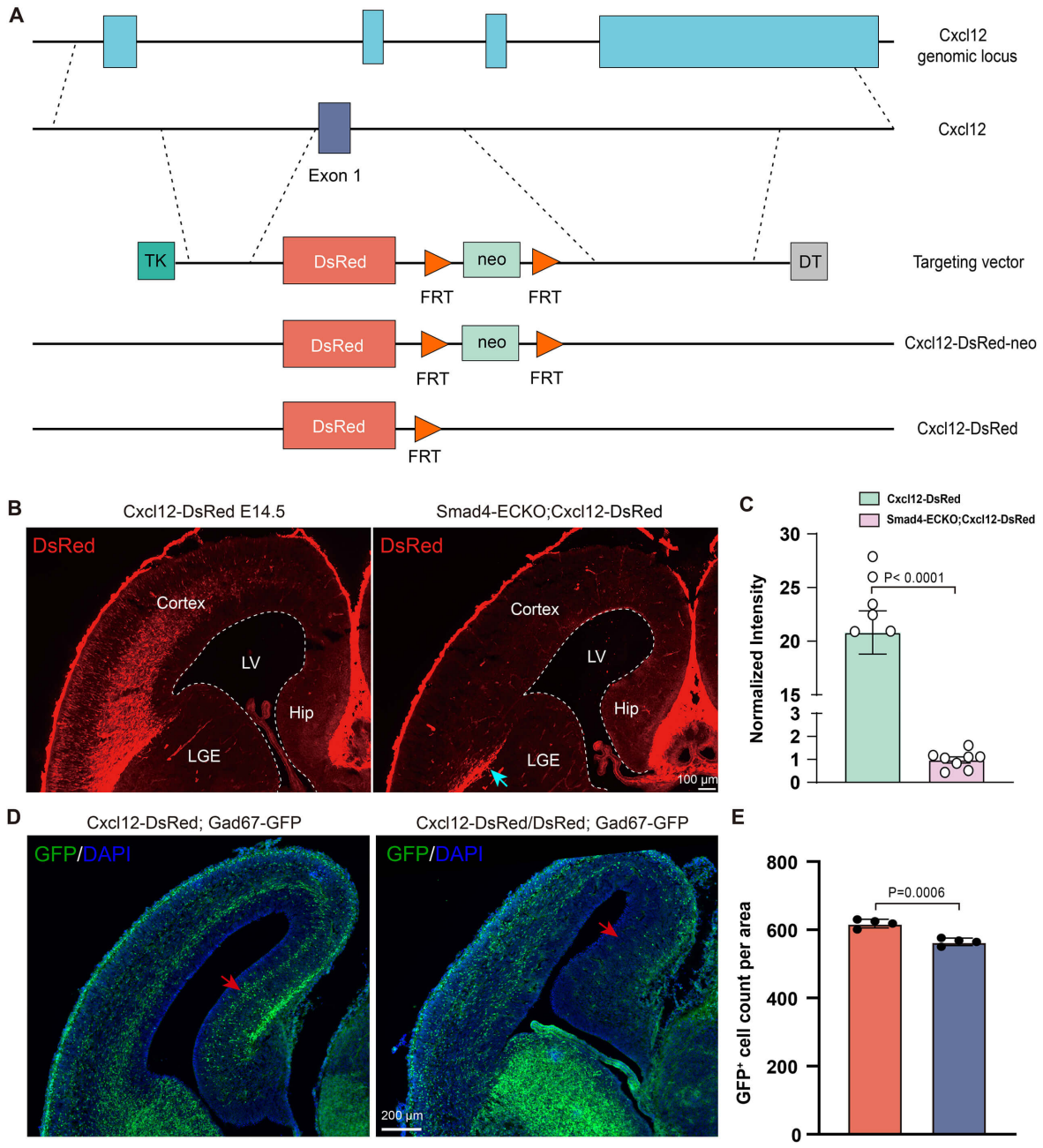


Fig. 3. Validation of Cxcl12 downregulation and its phenotypic mimicry of *Smad4* deficiency. (A) Schematic illustration of the targeting vector used to generate the Cxcl12-DsRed allele via recombineering. The vector was modified by inserting a DsRedE2-polyA-FRT-Neo-Frt cassette into the second exon of Cxcl12. (B) Representative immunofluorescence images demonstrating that, compared to Cxcl12-DsRed heterozygotes, DsRed signal (red fluorescence) is significantly reduced in the cortices of *Smad4*-ECKO; Cxcl12-DsRed mice at E14.5. This indicates a near-complete loss of Cxcl12 expression following cortical *Smad4* deletion. The dashed lines indicate anatomical boundaries. Cortex, LV, Hip, and LGE are labeled. Scale bar = 100 μm. (C) Bar graph showing the normalized DsRed fluorescence intensity ratio in the cortices of Cxcl12-DsRed and *Smad4*-ECKO; Cxcl12-DsRed mice. The significant reduction in fluorescence intensity further validates the scRNA-seq results. Due to the variability in fluorescence intensity, 6 mice were analyzed for the control group and 8 mice for the experimental group. (D) Representative immunohistochemical images showing that, compared to Cxcl12-DsRed heterozygotes, Cxcl12-DsRed/DsRed homozygous mice (Cxcl12 loss-of-function model) exhibit a significant reduction in the number of Gad67-GFP$^+$ cells in the cortex, mimicking the *Smad4* mutant phenotype. Note the marked decrease of Gad67-GFP$^+$ cells in the area indicated by the red arrow. Scale bar = 200 μm. (E) Quantification of GFP$^+$ cells in the cortex for the indicated genotypes. Data are presented as mean ± SEM (n = 4 mice per group); unpaired Student's *t*-test. DsRed, Discosoma red fluorescent protein; TK, Thymidine Kinase; FRT, Flippase Recognition Target/FLP Recombination Target.

Conversely, the transcription of the cognate receptor, Cxcr4, was completely preserved within the migrating interneuron population (Fig. 2E,F).

3.3 The Smad4-CXCL12 Axis Regulates Interneuron Positioning

To validate our scRNA-seq results *in vivo*, we used a Cxcl12-Discosoma red fluorescent protein (DsRed) knock-in reporter line generated via recombineering (Fig. 3A). At E14.5, *Smad4*-ECKO; Cxcl12-DsRed mice showed a clear reduction in cortical DsRed fluorescence, confirming that the loss of *Smad4* leads to a profound decrease in Cxcl12 expression at the proteidirectsn level (Fig. 3B,C). Next, we asked whether this reduction in CXCL12 is the primary driver of the observed interneuron phenotype. By examining Cxcl12-DsRed/DsRed homozygous mice (which act as a Cxcl12 loss-of-function model), we found a similar, significant reduction in cortical Gad67-GFP$^+$ interneurons, essentially phenocopying the *Smad4*-ECKO mutants (Fig. 3D,E). Together, these results indicate that *Smad4* participates in the regulation of cortical interneuron migration and distribution by controlling Cxcl12 expression.

4. Discussion

The precise assembly of cortical circuits requires intricate coordination between locally generated projection neurons (PNs) and tangentially migrating interneurons (INs). Emerging evidence indicates that pyramidal neuron identity is instructive for the subtype composition and integration of cortical interneurons [24]. Building upon this paradigm, our findings reveal that pallial progenitor function extends beyond mere structural scaffolds; they actively regulate the local chemotactic microenvironment. Specifically, we demonstrate that PN-derived *Smad4* dictates the intracortical progression of CXCR4-dependent INs by sustaining targeted CXCL12 secretion from intermediate progenitor cells (IPCs).

Critically, the pronounced reduction of cortical INs in *Smad4*-deficient mice reflects a primary failure in spatial recruitment rather than a depletion of the neurogenic lineage. Morphological assessments demonstrate an ectopic accumulation of mutant INs at the pallial-subpallial boundary (LGE), indicative of a developmental arrest prior to pallial entry. Meanwhile, both histological and scRNA-seq analyses confirm that the structural and transcriptomic fidelity of the glutamatergic progenitor pools (Pax6$^+$ radial glia and Eomes$^+$ IPCs) remains robustly preserved. These observations collectively confirm that interneuron generation and survival are intact, yet their migratory trajectory is fundamentally disrupted.

Mechanistically, this migratory arrest originates from a profound state of "ligand deprivation". While migrating INs maintain stable Cxcr4 expression, the drastic downregulation of IPC-derived CXCL12 precludes adequate receptor activation. This deficiency likely attenuates critical downstream effector cascades, including the phosphoinositide 3-kinase (PI3K)/protein kinase B(AKT) and Rho GTPase (e.g., Ras-related C3 botulinum toxin substrate 1 (Rac1)/cell division cycle 42 (Cdc42)) pathways, which are strictly required for cytoskeletal remodeling and directional motility [25]. The subset of INs that successfully populate the mutant cortex suggests the involvement of parallel compensatory mechanisms, potentially mediated by the atypical receptor CXCR7 [1,23,26,27,28] or redundant morphogenic cues such as neuregulin 1 (NRG1) [29] and hepatocyte growth factor (HGF) [30].

Beyond intracortical guidance, the *Smad4*-CXCL12 signaling cascade contributes to the macroscopic architecture of the developing brain. Ependymal cells line the brain ventricles and play important roles in maintaining cerebrospinal fluid homeostasis and barrier functions [31]. Given that Cxcl12 is endogenously expressed in the ependymal lining of the ventricles [32], its systemic depletion likely compromises the physical and functional boundaries of the neurogenic niche. This structural vulnerability provides a mechanistic basis for the ventriculomegaly observed in both *Smad4*-ECKO and Cxcl12 mutant brains, underscoring the dual requirement of the *Smad4*-CXCL12 axis in mediating both targeted cellular migration and overall cortical morphogenesis.

5. Limitations

Despite these insights, our study has several limitations that warrant future investigation. First, while we demonstrate that SMAD4 is essential for *Cxcl12* expression in intermediate progenitors, the exact molecular mechanism—whether SMAD4 directly binds to the *Cxcl12* regulatory elements or acts indirectly through intermediate transcription factors—remains to be elucidated. Second, our scRNA-seq analysis was conducted at a single embryonic stage (E14.5). Given the highly dynamic nature of cortical development, longitudinal transcriptomic profiling across multiple developmental time points is needed to fully capture the temporal evolution of these signaling landscapes. Finally, although a subset of interneurons successfully populated the mutant cortex, leading us to postulate the involvement of compensatory cues such as CXCR7 or NRG1, the exact functional redundancy of these parallel pathways requires further functional validation using double-knockout models in the future.

6. Conclusion

In conclusion, our study reveals a critical role for SMAD4 in orchestrating cortical development through the regulation of intermediate progenitor-derived CXCL12. We demonstrate that this SMAD4-CXCL12 signaling axis is essential for guiding the directed migration of interneurons into the developing mammalian cortex. By uncovering this specific molecular mechanism, our findings provide new insights into the dynamic interplay between pro-

jection neuron precursors and invading interneurons. Together, these results establish SMAD4 as a key regulator of cortical cytoarchitecture and cellular migration, offering a valuable framework for understanding the complex signaling landscapes that govern brain development and morphogenesis.

Availability of Data and Materials

The data that support the findings of this study are available from the corresponding authors upon reasonable request.

Author Contributions

YW designed the research, collected and analyzed the experimental data, and drafted the initial manuscript. YZ, YYL, YMW, WZH, and BQS assisted in experimental operation, data collation, and manuscript revision. BC and RLG conceived and supervised the research project, provided funding support, revised the manuscript critically for important intellectual content, and were responsible for the final approval of the version to be published. BC and RLG also served as corresponding authors for correspondence. All authors read and approved the final manuscript. All authors have participated sufficiently in the work and agreed to be accountable for all aspects of the work.

Ethics Approval and Consent to Participate

All mouse experimental procedures were performed in compliance with the National Institutes of Health Guide for the Care and Use of Laboratory Animals and the ARRIVE guidelines, and were approved by the Animal Ethics Committee of the Affiliated Hospital of Hebei University of Engineering (Approval No.: IACUC-Hebeu-2025-0020).

Acknowledgment

We are grateful to Professor Zhengang Yang from Fudan University for providing the *Smad4* floxed mice.

Funding

This work was supported by grants from the National Natural Science Foundation of China (No. 82501435), the Natural Science Foundation of Hebei Province (No. H2025402018), and the Medical Science Research Project of Hebei (No. 20250165).

Conflicts of Interest

The authors declare no conflicts of interest.

Supplementary Material

Supplementary material associated with this article can be found, in the online version, at https://doi.org/10.31083/JIN52364.

References

[1] Wang Y, Li G, Stanco A, Long JE, Crawford D, Potter GB, et al. CXCR4 and CXCR7 have distinct functions in regulating interneuron migration. Neuron. 2011; 69: 61–76. https://doi.org/10.1016/j.neuron.2010.12.005

[2] Sun L, Xiong F, Huang F, Dong S, Zhu P, Jiang P, et al. Transcriptomic insights into fate choice of pallial versus subpallial GABAergic neurons. Nature Communications. 2025; 16: 5032. https://doi.org/10.1038/s41467-025-60338-8

[3] Marín O, Rubenstein JLR. Cell migration in the forebrain. Annual Review of Neuroscience. 2003; 26: 441–483. https://doi.org/10.1146/annurev.neuro.26.041002.131058

[4] Abe P, Molnár Z, Tzeng YS, Lai DM, Arnold SJ, Stumm R. Intermediate Progenitors Facilitate Intracortical Progression of Thalamocortical Axons and Interneurons through CXCL12 Chemokine Signaling. The Journal of Neuroscience : the Official Journal of the Society for Neuroscience. 2015; 35: 13053–13063. https://doi.org/10.1523/JNEUROSCI.1488-15.2015

[5] Venkataramanappa S, Saaber F, Abe P, Schütz D, Kumar PA, Stumm R. Cxcr4 and Ackr3 regulate allocation of caudal ganglionic eminence-derived interneurons to superficial cortical layers. Cell Reports. 2022; 40: 111157. https://doi.org/10.1016/j.celrep.2022.111157

[6] Kawaguchi-Niida M, Shibata N, Furuta Y. Smad4 is essential for directional progression from committed neural progenitor cells through neuronal differentiation in the postnatal mouse brain. Molecular and Cellular Neurosciences. 2017; 83: 55–64. https://doi.org/10.1016/j.mcn.2017.06.008

[7] Colak D, Mori T, Brill MS, Pfeifer A, Falk S, Deng C, et al. Adult neurogenesis requires Smad4-mediated bone morphogenic protein signaling in stem cells. The Journal of Neuroscience : the Official Journal of the Society for Neuroscience. 2008; 28: 434–446. https://doi.org/10.1523/JNEUROSCI.4374-07.2008

[8] Naik AS, Lin JM, Taroc EZM, Katreddi RR, Frias JA, Lemus AA, et al. Smad4-dependent morphogenic signals control the maturation and axonal targeting of basal vomeronasal sensory neurons to the accessory olfactory bulb. Development (Cambridge, England). 2020; 147: dev184036. https://doi.org/10.1242/dev.184036

[9] Del-Valle-Anton L, Amin S, Cimino D, Neuhaus F, Dvoretskova E, Fernández V, et al. Multiple parallel cell lineages in the developing mammalian cerebral cortex. Science Advances. 2024; 10: eadn9998. https://doi.org/10.1126/sciadv.adn9998

[10] Yang X, Li C, Herrera PL, Deng CX. Generation of Smad4/Dpc4 conditional knockout mice. Genesis (New York, N.Y. : 2000). 2002; 32: 80–81. https://doi.org/10.1002/gene.10029

[11] Tian Y, Wang Z, Yang F, Zhang W, Li J, Yang L, et al. Olig1/2 Orchestrates Progenitor Cell Fates during Mammalian Cortical Gliogenesis and Gliomagenesis. Nature Communications. 2025; 16: 9779. https://doi.org/10.1038/s41467-025-64753-9

[12] Wang Z, Tian Y, Fu T, Yang F, Li J, Yang L, et al. Coordinated regulation of cortical astrocyte maturation by OLIG1 and OLIG2 through BMP7 signaling modulation. Journal of Genetics and Genomics = Yi Chuan Xue Bao. 2025; 52: 1224–1237. https://doi.org/10.1016/j.jgg.2025.03.008

[13] Oliva AA, Jr, Jiang M, Lam T, Smith KL, Swann JW. Novel hippocampal interneuronal subtypes identified using transgenic mice that express green fluorescent protein in GABAergic interneurons. The Journal of Neuroscience : the Official Journal of the Society for Neuroscience. 2000; 20: 3354–3368. https://doi.org/10.1523/JNEUROSCI.20-09-03354.2000

[14] Ding L, Morrison SJ. Haematopoietic stem cells and early lymphoid progenitors occupy distinct bone marrow niches. Nature. 2013; 495: 231–235. https://doi.org/10.1038/nature11885

[15] Zhang Z, Xu Z, Fu T, Li J, Yang F, Yang C, et al. Integrated ERK-PKA-YAP/TAZ-SHH Signaling Orchestrates Cortical Ra-

dial Glia Identity and Lineage Diversification. Advanced Science (Weinheim, Baden-Wurttemberg, Germany). 2026; 13: e13571. https://doi.org/10.1002/advs.202513571

[16] Angara K, Pai ELL, Bilinovich SM, Stafford AM, Nguyen JT, Li KX, et al. *Nf1* deletion results in depletion of the *Lhx6* transcription factor and a specific loss of parvalbumin^{+} cortical interneurons. Proceedings of the National Academy of Sciences of the United States of America. 2020; 117: 6189–6195. https://doi.org/10.1073/pnas.1915458117

[17] Ibrahim LA, Schuman B, Bandler R, Rudy B, Fishell G. Mining the jewels of the cortex's crowning mystery. Current Opinion in Neurobiology. 2020; 63: 154–161. https://doi.org/10.1016/j.conb.2020.04.005

[18] Alifragis P, Liapi A, Parnavelas JG. Lhx6 regulates the migration of cortical interneurons from the ventral telencephalon but does not specify their GABA phenotype. The Journal of Neuroscience : the Official Journal of the Society for Neuroscience. 2004; 24: 5643–5648. https://doi.org/10.1523/JNEUROSCI.1245-04.2004

[19] Mayer C, Hafemeister C, Bandler RC, Machold R, Batista Brito R, Jaglin X, et al. Developmental diversification of cortical inhibitory interneurons. Nature. 2018; 555: 457–462. https://doi.org/10.1038/nature25999

[20] Toritsuka M, Kimoto S, Muraki K, Landek-Salgado MA, Yoshida A, Yamamoto N, et al. Deficits in microRNA-mediated Cxcr4/Cxcl12 signaling in neurodevelopmental deficits in a 22q11 deletion syndrome mouse model. Proceedings of the National Academy of Sciences of the United States of America. 2013; 110: 17552–17557. https://doi.org/10.1073/pnas.1312661110

[21] Marín O. Cellular and molecular mechanisms controlling the migration of neocortical interneurons. The European Journal of Neuroscience. 2013; 38: 2019–2029. https://doi.org/10.1111/ejn.12225

[22] Tiveron MC, Rossel M, Moepps B, Zhang YL, Seidenfaden R, Favor J, et al. Molecular interaction between projection neuron precursors and invading interneurons via stromal-derived factor 1 (CXCL12)/CXCR4 signaling in the cortical subventricular zone/intermediate zone. The Journal of neuroscience: the official journal of the Society for Neuroscience. 2006; 26: 13273–13278. https://doi.org/10.1523/JNEUROSCI.4162-06.2006

[23] Abe P, Mueller W, Schütz D, MacKay F, Thelen M, Zhang P, et al. CXCR7 prevents excessive CXCL12-mediated down-regulation of CXCR4 in migrating cortical interneurons. Development (Cambridge, England). 2014; 141: 1857–1863. https://doi.org/10.1242/dev.104224

[24] Wu SJ, Dai M, Yang SP, McCann C, Qiu Y, Kumar V, et al. Pyramidal neurons proportionately alter cortical interneuron subtypes. Nature. 2026; 651: 421–428. https://doi.org/10.1038/s41586-025-09996-8

[25] Danuser G, Allard J, Mogilner A. Mathematical modeling of eukaryotic cell migration: insights beyond experiments. Annual Review of Cell and Developmental Biology. 2013; 29: 501–528. https://doi.org/10.1146/annurev-cellbio-101512-122308

[26] Sánchez-Alcañiz JA, Haege S, Mueller W, Pla R, Mackay F, Schulz S, et al. Cxcr7 controls neuronal migration by regulating chemokine responsiveness. Neuron. 2011; 69: 77–90. https://doi.org/10.1016/j.neuron.2010.12.006

[27] Shi Y, Riese DJ, 2nd, Shen J. The Role of the CXCL12/CXCR4/CXCR7 Chemokine Axis in Cancer. Frontiers in Pharmacology. 2020; 11: 574667. https://doi.org/10.3389/fphar.2020.574667

[28] Guyon A. CXCL12 chemokine and its receptors as major players in the interactions between immune and nervous systems. Frontiers in Cellular Neuroscience. 2014; 8: 65. https://doi.org/10.3389/fncel.2014.00065

[29] Flames N, Long JE, Garratt AN, Fischer TM, Gassmann M, Birchmeier C, et al. Short- and long-range attraction of cortical GABAergic interneurons by neuregulin-1. Neuron. 2004; 44: 251–261. https://doi.org/10.1016/j.neuron.2004.09.028

[30] Powell EM, Mars WM, Levitt P. Hepatocyte growth factor/scatter factor is a motogen for interneurons migrating from the ventral to dorsal telencephalon. Neuron. 2001; 30: 79–89. https://doi.org/10.1016/s0896-6273(01)00264-1

[31] Maugeri G, Amato A, Evola G, D'Agata V, Musumeci G. Addressing the Effect of Exercise on Glial Cells: Focus on Ependymal Cells. Journal of Integrative Neuroscience. 2024; 23: 216. https://doi.org/10.31083/j.jin2312216

[32] Eisa-Beygi S, Arulsamy K, Cui K, Wu H, Wang B, Chen K, et al. The chemokine receptor CXCR4 and its ligand CXCL12 (SDF-1) localize to ependymal cilia in brain ventricles. Vascular Pharmacology. 2025; 161: 107546. https://doi.org/10.1016/j.vph.2025.107546